A New Measurement of $\Xi^- \to \Lambda\pi^-$ Decay Parameters

M. Huang,[10] R. A. Burnstein,[5] A. Chakravorty,[5] Y. C. Chen,[1] W. S. Choong,[2,7] K. Clark,[9] E. C. Dukes,[10] C. Durandet,[10] J. Felix,[4] G. Gidal,[7] H. R. Gustafson,[8] T. Holmstrom,[10] C. James,[3] C. M. Jenkins,[9] T. Jones,[7] D. M. Kaplan,[5] L. M. Lederman,[5] N. Leros,[6] M. J. Longo,[8] Fred Lopez,[8] L. Lu,[10] W. Luebke,[5] K.B. Luk,[2,7] K. S. Nelson,[10] H. K. Park,[8] J. P. Perroud,[6] D. Rajaram,[5,8] H. A. Rubin,[5] J. Volk,[3] C. White,[5] S. White,[5] and P. Zyla[7]

(HyperCP Collaboration)

[1]*Institude of Physics, Academia Sinica, Taipei 11529, Taiwan, Republic of China*

[2]*University of California, Berkeley, CA 94720*

[3]*Fermi National Accelerator Laboratory, Batavia, IL 60510*

[4]*University of Guanajuato, 37000 Leon, Mexico*

[5]*Illinois Institute of Technology, Chicago, IL 60616*

[6]*University of Lausanne, CH-1015 Lausanne, Switzerland*

[7]*Lawrence Berkeley National Laboratory, Berkeley, CA 94720*

[8]*University of Michigan, Ann Arbor, MI 48109*

[9]*University of South Alabama, Mobile, AL 36688*

[10]*University of Virginia, Charlottesville, VA 22904*

Based on a sample of 144×10^6 polarized $\Xi^-\to\Lambda\pi^-, \Lambda\to p\pi^-$ decays collected by the HyperCP experiment (E871) at Fermilab, we report a new measurement of the Ξ^- decay-parameter angle $\phi_\Xi = (-2.39\pm0.64\pm0.64)^\circ$ from which we deduce the decay parameters $\beta_\Xi = -0.037\pm0.011\pm0.010$ and $\gamma_\Xi = 0.888\pm0.0004\pm0.006$. Assuming that the CP-violating phase difference between s and p waves is negligible, the strong phase-shift difference, $\delta_p-\delta_s$, for $\Lambda\pi$ scattering is determined to be $(4.6\pm1.4\pm1.2)^\circ$.

PACS numbers: 13.30.Eg, 11.30.Er, 14.20.Jn, 14.65.Bt

It was suggested in [1] that differing angular distributions in hyperon and antihyperon nonleptonic decay modes would provide evidence of CP violation. The decay of a spin-$\frac{1}{2}$ hyperon into a baryon and pion contains a mixture of s- and p-waves whose amplitudes (s, p) can be used to describe the angular distribution with the parameters $\alpha = 2\mathrm{Re}(s^*p)/(|s^2|+|p^2|)$, $\beta = 2\mathrm{Im}(s^*p)/(|s^2|+|p^2|)$, and $\gamma = (|s^2|-|p^2|)/(|s^2|+|p^2|)$ [2, 3]. Subsequent experiments [4] compared the parity-violating decay parameter α_Y for a given hyperon species Y to that of the corresponding antihyperon $\alpha_{\overline{Y}}$ via an asymmetry, which for $\Xi^-\to\Lambda\pi^-$ is given by

$$\mathcal{A}_\Xi = \frac{\alpha_\Xi+\alpha_{\overline{\Xi}}}{\alpha_\Xi-\alpha_{\overline{\Xi}}}\,. \tag{1}$$

A model-independent approximation for $\mathcal{A}_\Xi$ is [5]

$$\mathcal{A}_\Xi = -\tan(\delta_p-\delta_s)\sin(\phi_p-\phi_s)\,, \tag{2}$$

where $\delta_p-\delta_s$ is the difference between the p- and s-wave $\Lambda\pi$ final-state scattering phase-shifts and $\phi_p-\phi_s$ is the (CP-violating) difference between weak-interaction phases in the decay. To set limits on the observability of $\mathcal{A}_\Xi$ one needs a measurement of the final-state phase-shifts. Theoretical predictions of $\delta_p-\delta_s$ vary between -3° and 16° [6]. Measurement of the $\Lambda\pi$ final-state phase-shifts from elastic scattering, e.g. as done in [7] for $\Lambda\to p\pi$, is impractical. However, if the weak-interaction phase difference is negligible compared to that of the strong phase-shift, $\delta_p-\delta_s$ can be determined through the ratio [8]

$$\frac{\beta_\Xi}{\alpha_\Xi} = \tan(\delta_p-\delta_s)\,. \tag{3}$$

The decay parameter β_Ξ is usually specified together with γ_Ξ as an angle $\phi_\Xi = \tan^{-1}(\beta_\Xi/\gamma_\Xi)$. Using the world average [9] of $\phi_\Xi = (4\pm4)^\circ$ the value of $\delta_p-\delta_s$ is found to be $(-7.8\pm7.8)^\circ$. Recently E756 [10] obtained $\delta_p-\delta_s = (3.17\pm5.28\pm0.73)^\circ$ based on 1.35 million polarized Ξ^- events. In this letter, we report a measurement of ϕ_Ξ from which we extract $\delta_p-\delta_s$ based on a data set of 144 million polarized $\Xi^-\to\Lambda\pi^-$ decays collected in the HyperCP experiment.

The HyperCP experiment was designed primarily to search for CP violation in $\Xi^-/\overline{\Xi}^+$ and $\Lambda/\overline{\Lambda}$ decays. Data were collected in the Meson Center beam line at Fermilab in 1997 and 1999. The analysis reported here used polarized Ξ^- data from 1999. A plan view of the spectrometer is shown in Fig. 1 .

Polarized Ξ^-'s were produced by directing an 800-GeV/c proton beam onto a 2 mm × 2 mm × 60 mm copper target at angles of +3 and −3 mrad in the horizontal plane with respect to the axis of a 6.096 m-long collimator located within a dipole magnet (Hyperon Magnet). The Hyperon Magnet had a field integral of 10.18 ± 0.03 T-m and deflected the beam upward by approximately 19 mrad. The mean momentum of the secondary beam was 163 GeV/c. Within the collimator a moving

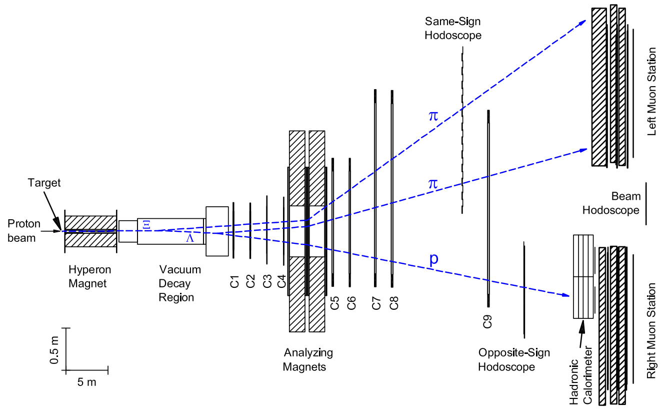

FIG. 1: Plan view of the HyperCP spectrometer. The length (width) of the spectrometer is about 62 m (4 m).

coordinate system was employed in which $\hat{z}$ was tangent to the nominal central orbit and $\hat{y}$ pointed toward the center of curvature. At the entrance of the collimator (and at the target) $\hat{y}$ was vertical. A positive production angle was defined by $(\hat{p}_{\rm beam} \times \hat{z}) \cdot \hat{y} > 0$, where $\hat{p}_{\rm beam}$ is a unit vector in the direction of the incident proton. Most of the Ξ^-'s that emerged from the collimator exit decayed inside a 13 m-long vacuum pipe (Decay Region) immediately downstream of the collimator. Following the Decay Region were nine multiwire proportional chambers (C1–C9). An analyzing magnet comprising two dipoles deflected charged particles horizontally with a transverse-momentum kick of 1.43 GeV/c. Particles having the same charge as the Ξ^-'s were deflected towards $+x$ and those having opposite charge towards $-x$. At the downstream end of the spectrometer were two scintillation hodoscopes and a calorimeter, used for triggering, and a muon detector system, used for muonic rare-decay studies.

The reconstructed events were required to have three tracks and satisfy a two-vertex topology corresponding to the Ξ^- decay sequence hypothesis. The proton and pion from the Λ decay were required to have a $p\pi$ invariant mass within 3.5 standard deviations ($\pm 3.5\,{\rm MeV}/c^2$) of the Λ mass peak at 1.116 GeV/c^2, and the $p\pi\pi$ invariant mass was required to be within 3.2 standard deviations ($\pm 5.6\,{\rm MeV}/c^2$) of the Ξ^- mass peak at 1.322 GeV/c^2. The momenta of the reconstructed Ξ^- candidates were required to be between 110 and 240 GeV/c. The Λ decay vertex was required to be downstream of the Ξ^- decay vertex, and both vertices were required to be in a 12.7-m-long fiducial region within the vacuum pipe extending from 30 cm downstream of the collimator exit to 89 cm upstream of C1.

In the decay sequence $\Xi^- \to \Lambda\pi^-$, $\Lambda \to p\pi^-$ the joint distribution function for the decay has the form [3]

$$\frac{d^2N}{d\Omega_\Lambda\, d\Omega_p} = \frac{1}{(4\pi)^2}(1+\alpha_\Xi \vec{P}_\Xi \cdot \hat{\Lambda})(1+\alpha_\Lambda \vec{P}_\Lambda \cdot \hat{p}) \,, \quad (4)$$

where $\hat{\Lambda}$ and $\hat{p}$ are the momentum unit vectors of the Λ in the Ξ^- rest frame and the proton in the Λ rest frame. $\vec{P}_\Xi$ and $\vec{P}_\Lambda$ are the polarizations of the Ξ^- and Λ which are related by [3]

$$\vec{P}_\Lambda = \frac{(\alpha_\Xi + \vec{P}_\Xi \cdot \hat{\Lambda})\hat{\Lambda} + \beta_\Xi(\vec{P}_\Xi \times \hat{\Lambda}) + \gamma_\Xi \hat{\Lambda} \times (\vec{P}_\Xi \times \hat{\Lambda})}{1+\alpha_\Xi \vec{P}_\Xi \cdot \hat{\Lambda}} \,. \quad (5)$$

The helicity-frame axes, specified event-by-event in the Λ rest frame, are defined as

$$\hat{z}' = \hat{\Lambda} \,, \quad \hat{x}' = \frac{\vec{P}_\Xi \times \hat{\Lambda}}{|\vec{P}_\Xi \times \hat{\Lambda}|} \,, \quad \hat{y}' = \hat{z}' \times \hat{x}' \,. \quad (6)$$

After an azimuthal integration of $\hat{p}$ in Eq. 4 around the z' axis the terms dependent on β_Ξ and γ_Ξ vanish and the joint distribution becomes

$$\frac{d^2N}{d\Omega_\Lambda\, d\cos\theta_{pz'}} = \frac{1}{8\pi}\left[(1+\alpha_\Xi \vec{P}_\Xi \cdot \hat{\Lambda}) + \alpha_\Lambda(\alpha_\Xi + \vec{P}_\Xi \cdot \hat{\Lambda})\cos\theta_{pz'}\right] . (7)$$

After an integration over all directions of the Λ in the Ξ^- rest frame the distribution of the proton with respect to $\hat{x}'$ ($\hat{y}'$) in the Λ rest frame is given by

$$\frac{dN}{d\cos\theta_{px'}} = \frac{1}{2}(1+\frac{\pi}{4}\alpha_\Lambda\beta_\Xi P_\Xi \cos\theta_{px'}) \quad (8)$$

$$\frac{dN}{d\cos\theta_{py'}} = \frac{1}{2}(1+\frac{\pi}{4}\alpha_\Lambda\gamma_\Xi P_\Xi \cos\theta_{py'}) \,, \quad (9)$$

where P_Ξ is the magnitude of the Ξ^- polarization and $\theta_{px'}$ ($\theta_{py'}$) is the angle between the proton momentum in the Λ rest frame and the x' (y') axis. In the following analysis the three components of $\vec{P}_\Xi$ were measured using Eq. 7 while Eqs. 8 and 9 were used in the measurements of the products $\frac{\pi}{4}\alpha_\Lambda\beta_\Xi P_\Xi$ and $\frac{\pi}{4}\alpha_\Lambda\gamma_\Xi P_\Xi$.

A Hybrid Monte Carlo (HMC) technique [11] was employed to measure the polarization of Ξ^-'s decaying in the Decay Region. For each real event HMC events were generated uniformly in $\cos\theta_{pz'}$, passed through a simulation of the apparatus, reconstructed and subjected to the same event selection requirements as the real data until ten HMC events were accepted. The HMC events were weighted by a ratio of the expected angular distribution (Eq. 7) evaluated at the generated angle to that evaluated at the original angle. In this ratio the polarization was considered as a parameter that was varied to minimize the deviation of the weighted HMC angular distribution from that of the real data. The quantity extracted from the fit was the sum of the true polarization plus a bias which resulted from systematic effects not fully accounted for in the HMC. Since the sign of the polarization changed with the sign of the production angle while that of the bias did not, two nonzero-production-angle (± 3 mrad) data samples were used to extract [12] the true polarization and the bias. The results are listed in Table I in five equally populated Ξ^- momentum bins, whose central values appear in the first column. These biases were consistent with the signal extracted from an unpolarized sample.

The x component of the Ξ^- polarization for the entire data sample was found to be 0.0001 ± 0.0005, in good agreement with zero as expected from parity conservation in the strong production process. Over the range of Ξ^- momentum (p_Ξ) accessible to the experiment, the major (y) component of the polarization was found to be well described by a linear parameterization, $P_{\Xi y} = \pm 0.027 \mp 0.00039(\mathrm{GeV}^{-1}) \times p_\Xi$, where the upper (lower) sign applies to the positive (negative) production angle data sample. The z component of the polarization exhibited a similar trend. Due to precession of the Ξ^- spins in the x-directed field of the Hyperon Magnet a non-zero z component of polarization arose in the Decay Region from the initially y-directed polarization at the target. The precession angle, $\Psi = \arctan(P_{\Xi z}/P_{\Xi y})$, was determined for each momentum bin and the values were found to be independent of the Ξ^- momentum and have an average of $(10.04 \pm 0.92)^\circ$. As a check the magnetic moment was deduced to be $\mu_\Xi = -0.6562 \pm 0.0051(\mathrm{stat})\ \mu_N$, consistent with the world average $-0.6507 \pm 0.0025\ \mu_N$ [9].

The measurements of the products $\frac{\pi}{4}\alpha_\Lambda \beta_\Xi P_\Xi$ and $\frac{\pi}{4}\alpha_\Lambda \gamma_\Xi P_\Xi$ also employed the HMC method with weighting functions based, respectively, on Eqs. 8 and 9. To determine the x' and y' axes (Eq. 6) along which the proton direction should be projected, each event was assigned polarization components: $P_{\Xi x} = 0$, $P_{\Xi y}$ from the linear parameterization given above and $P_{\Xi z} = P_{\Xi y} \tan \Psi$. Figure 2 shows the distributions of $\cos\theta_{px'}$ and $\cos\theta_{py'}$ for real events and the corresponding weighted HMC events for the two production angles. The true products were separated from the biases by combining results from the positive and negative production angles as in [10]. The measured products and biases as a function of p_Ξ are listed in Table II. The angle ϕ_Ξ deduced from the ratio of these products is listed in the last column of the same table. For comparison with the final results given later we note that the decay parameters β_Ξ and γ_Ξ could be deduced (albeit with larger errors) from these measured products after division by $\frac{\pi}{4}\alpha_\Lambda = 0.504 \pm 0.010$ [9] and P_Ξ from Table I. These values exhibited no significant dependence on p_Ξ and the averages over the momentum range were $\langle \beta_\Xi \rangle = -0.037 \pm 0.010$ and $\langle \gamma_\Xi \rangle = 0.889 \pm 0.009$, where the errors are statistical.

The sources of systematic uncertainties in the measurements of the products $\frac{\pi}{4}\alpha_\Lambda \beta_\Xi P_\Xi$ and $\frac{\pi}{4}\alpha_\Lambda \gamma_\Xi P_\Xi$ can be separated into four categories: background events, event selection, detector simulation and polarization uncertainties.

The HMC generated only Ξ^- decays while the real data contained roughly 0.4% background events. The ef-

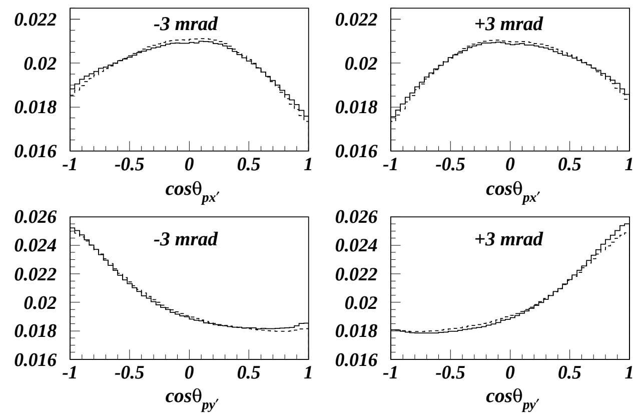

FIG. 2: Proton $\cos\theta_{px'}$ and $\cos\theta_{py'}$ distributions; the solid line is real events, and the dashed line is weighted HMC events.

fect of these background events on the measurements was estimated by analyzing events well above and below the Ξ^- mass peak and weighting the deviation from the nominal values by the extrapolated fraction of background events under the peak. The other categories of systematic uncertainties were estimated by varying selection criteria or parameters in the analysis and reanalyzing the data sample. Selection cuts on event parameters such as vertex locations were tightened by one standard deviation of the resolution function. Included in the event-selection cuts were tighter fiducial cuts on the active volumes of wire chambers and the aperture of the analyzing magnets which reduced the acceptance by roughly 7%. The HMC (fake) protons and pions were propagated through a simulation of the apparatus in which they deposited hits in the hodoscopes, calorimeter and MWPCs with efficiencies obtained from real data. To estimate the sensitivity of the measurement to the detector efficiencies, the latter were varied by amounts obtained from small changes to the algorithms used in their determination. The HMC events contained only the detector hits due to the real Ξ^- pion and the fake proton and pion. To estimate the sensitivity to accidental hits, each fake event was superimposed with detector hits from the real event which were not associated with the proton or pion. The contribution to the systematic error due to the polarization measurement was dominated by the uncertainty in the precession angle which was varied by ± 1 standard deviation (statistical) as given above.

Table III summarizes the contributions of the sources of systematic errors described above in units of the statistical error. Since ten accepted HMC events were generated for each real event there was a contribution to each systematic error source of approximately $\sigma_{\mathrm{stat}}/\sqrt{10}$. Therefore the systematic errors are somewhat overestimated. The total systematic error, which is shown in the last line of Table III, was estimated by adding the

p_Ξ (GeV/c)	$P_{\Xi x}$	$B_{P_{\Xi x}}$	$P_{\Xi y}$	$B_{P_{\Xi y}}$	$P_{\Xi z}$	$B_{P_{\Xi z}}$
139	-0.0011 ± 0.0011	0.0363	-0.0264 ± 0.0012	-0.0035	-0.0059 ± 0.0015	-0.0908
152	0.0010 ± 0.0011	0.0357	-0.0325 ± 0.0011	0.0023	-0.0059 ± 0.0014	-0.0880
162	0.0014 ± 0.0010	0.0288	-0.0340 ± 0.0010	-0.0026	-0.0047 ± 0.0013	-0.0833
173	-0.0006 ± 0.0010	0.0227	-0.0405 ± 0.0011	-0.0040	-0.0072 ± 0.0013	-0.0762
191	-0.0005 ± 0.0011	0.0177	-0.0467 ± 0.0013	-0.0132	-0.0087 ± 0.0013	-0.0710

TABLE I: Components of Ξ^- polarization in the Decay Region and the corresponding biases.

p_Ξ (GeV/c)	$\frac{\pi}{4}\alpha_\Lambda\beta_\Xi P_\Xi$	$B_{\frac{\pi}{4}\alpha_\Lambda\beta_\Xi P_\Xi}$	$\frac{\pi}{4}\alpha_\Lambda\gamma_\Xi P_\Xi$	$B_{\frac{\pi}{4}\alpha_\Lambda\gamma_\Xi P_\Xi}$	ϕ_Ξ (degree)
139	-0.00037 ± 0.00047	-0.00329	0.01191 ± 0.00041	0.00894	-1.77 ± 2.28
152	-0.00046 ± 0.00047	-0.00229	0.01447 ± 0.00038	0.00618	-1.81 ± 1.88
162	-0.00038 ± 0.00041	-0.00171	0.01557 ± 0.00035	0.00522	-1.39 ± 1.49
173	-0.00074 ± 0.00040	0.00034	0.01880 ± 0.00036	0.00729	-2.26 ± 1.22
191	-0.00123 ± 0.00040	0.00199	0.02109 ± 0.00040	0.00708	-3.33 ± 1.08

TABLE II: Measured $\frac{\pi}{4}\alpha_\Lambda\beta_\Xi P_\Xi$ and $\frac{\pi}{4}\alpha_\Lambda\gamma_\Xi P_\Xi$, the corresponding biases, and the deduced ϕ_Ξ.

Systematic source	$\frac{\pi}{4}\alpha_\Lambda\beta_\Xi P_\Xi$ ($\times 0.00019$)	$\frac{\pi}{4}\alpha_\Lambda\gamma_\Xi P_\Xi$ ($\times 0.00017$)
Accidental hits	0.28	0.06
Background	0.06	0.22
Detector efficiency	0.39	0.50
Precession angle	0.58	0.17
Event selection	0.61	0.64
Total error	0.97	0.86

TABLE III: Systematic errors for the measurement of $\frac{\pi}{4}\alpha_\Lambda\beta_\Xi P_\Xi$ and $\frac{\pi}{4}\alpha_\Lambda\gamma_\Xi P_\Xi$; all entries are in units of the statistical errors shown in parentheses.

individual contributions in quadrature.

The weighted average of ϕ_Ξ from Table II, with systematic uncertainties from Table III, was found to be

$$\phi_\Xi = [-2.39 \pm 0.64(\text{stat}) \pm 0.64(\text{syst})]^\circ \ .$$

This is consistent with the measurement in [10]. Using the identity $\alpha_\Xi^2 + \beta_\Xi^2 + \gamma_\Xi^2 = 1$ and the relatively well known (compared to the polarization uncertainties in this experiment) value of $\alpha_\Xi = -0.458 \pm 0.012$ [9] the decay parameters were calculated using

$$\beta_\Xi = \sqrt{1-\alpha_\Xi^2}\sin\phi_\Xi \ \text{ and } \ \gamma_\Xi = \sqrt{1-\alpha_\Xi^2}\cos\phi_\Xi \ .$$

The resulting values are

$$\begin{aligned} \beta_\Xi &= -0.037 \pm 0.011(\text{stat}) \pm 0.010(\text{syst}) \\ \gamma_\Xi &= \ \ 0.888 \pm 0.0004(\text{stat}) \pm 0.006(\text{syst}) \end{aligned}$$

where the systematic error includes the uncertainty of α_Ξ. Under the assumptions in Eq. 3, we then determine the strong phase-shift difference for $\Lambda\pi$ scattering to be :

$$\delta_p - \delta_s = (4.6 \pm 1.4 \pm 1.2)^\circ \ .$$

In conclusion, we have obtained a new measurement of ϕ_Ξ using a sample of 144 million $\Xi^- \to \Lambda\pi^-$ decays having an average polarization of 3.7%. This result, which is a 2.9× improvement over the best previous measurement [10], may indicate a non-zero value of β_Ξ. Assuming the validity of Eq. 3, this would imply that *CP* violation in charged $\Xi \to \Lambda\pi$ decays would not be suppressed by a vanishing final-state phase-shift difference.

We would like to acknowledge support by the U.S. Department of Energy. E.C.D. and K.S.N. were partially supported by the Institute for Nuclear and Particle Physics. The excellent assistance of the Fermilab staff for this experiment is gratefully acknowledged.

[1] A. Pais, Phys. Rev. Lett. **3**, 242 (1959).
[2] T. D. Lee *et al.*, Phys. Rev. **106**, 1367 (1957).
[3] T. D. Lee and C. N. Yang, Phys. Rev. **108**, 1645 (1957).
[4] P. Chauvat *et al.*, Phys. Lett. B **163**, 273 (1985); M. H. Tixier *et al.*, Phys. Lett. **212**, 523 (1988); P. D. Barnes *et al.*, Phys. Rev. C **54**, 1877 (1996); K. B. Luk *et al.*, Phys. Rev. Lett. **85**, 4860 (2000).
[5] J. F. Donoghue, X.-G. He, and S. Pakvasa, Phys. Rev. D **34**, 833 (1986).
[6] R. Nath, Nuovo Cimento **36**, 1949 (1965); M. Lu, M. Wise, and M. Savage, Phys. Lett. B **337**, 133 (1994); A. Datta and S. Pakvasa, Phys. Lett. B **344**, 430 (1995); A. Kamal, Phys. Rev. D **58**, 077501 (1998); U.-G. Meißner and J.A. Oller, Phys. Rev. D **64**, 014006 (2001); J. Tandean, A.W. Thomas, and G. Valencia, Phys. Rev. D **64**, 014005 (2001).
[7] L.D. Roper, R.M. Wright and B.T. Feld, Phys. Rev. **138**, B190 (1965).
[8] O. E. Overseth, Phys. Rev. Lett. **19**, 395 (1967).
[9] Particle Data Group, K. Hagiwara *et al.*, Phys. Rev. D **66** (2002).
[10] A. Chakravorty *et al.*, Phys. Rev. Lett. **91**, 031601 (2003).
[11] G. Bunce, Nucl. Instrum. Methods **172**, 533 (1980).
[12] R. Rameika *et al.*, Phys. Rev. D**33**, 3172 (1986).